Published in final edited form as:
Invest Radiol. 2013 January ; 48(1): . doi:10.1097/RLI.0b013e318271869c.

Free-Breathing Contrast-Enhanced Multiphase MRI of the Liver Using a Combination of Compressed Sensing, Parallel Imaging, and Golden-Angle Radial Sampling

Hersh Chandarana, MD, **Li Feng, MS**, **Tobias K. Block, PhD**, **Andrew B. Rosenkrantz, MD**, **Ruth P. Lim, MBBS, MMed, FRANZCR**, **James S. Babb, PhD**, **Daniel K. Sodickson, MD, PhD**, and **Ricardo Otazo, PhD**
Center for Biomedical Imaging, Department of Radiology, New York University Langone Medical Center, New York, NY.

Abstract

Objective—The objectives of this study were to develop a new method for free-breathing contrast-enhanced multiphase liver magnetic resonance imaging (MRI) using a combination of compressed sensing, parallel imaging, and radial k-space sampling and to demonstrate the feasibility of this method by performing image quality comparison with breath-hold cartesian T1-weighted (conventional) postcontrast acquisitions in healthy participants.

Materials and Methods—This Health Insurance Portability and Accountability Act–compliant prospective study received approval from the institutional review board. Eight participants underwent 3 separate contrast-enhanced fat-saturated T1-weighted gradient-echo MRI examinations with matching imaging parameters: conventional breath-hold examination with cartesian k-space sampling volumetric interpolate breath hold examination (BH-VIBE) and free-breathing acquisitions with interleaved angle-bisection and continuous golden-angle radial sampling schemes. Interleaved angle-bisection and golden-angle data from each 100 consecutive spokes were reconstructed using a combination of compressed sensing and parallel imaging (interleaved-angle radial sparse parallel [IARASP] and golden-angle radial sparse parallel [GRASP]) to generate multiple postcontrast phases.

Arterial- and venous-phase BH-VIBE, IARASP, and GRASP reconstructions were evaluated by 2 radiologists in a blinded fashion. The readers independently assessed quality of enhancement (QE), overall image quality (IQ), and other parameters of image quality on a 5-point scale, with the highest score indicating the most desirable examination. Mixed model analysis of variance was used to compare each measure of image quality.

Results—Images of BH-VIBE and GRASP had significantly higher QE and IQ values compared with IARASP for both phases ($P < 0.05$). The differences in QE between BH-VIBE and GRASP for the arterial and venous phases were not significant ($P > 0.05$). Although GRASP had lower IQ score compared with BH-VIBE for the arterial (3.9 vs 4.8; $P < 0.0001$) and venous (4.2 vs 4.8; $P = 0.005$) phases, GRASP received IQ scores of 3 or more in all participants, which was consistent with acceptable or better diagnostic image quality.

Reprints: Hersh Chandarana, MD, Department of Radiology, New York University Langone Medical Center, 550 First Ave, HW201, New York, NY 10016. hersh.chandarana@nyumc.org..

Conflicts of interest and sources of funding: none declared.

Conclusion—Contrast-enhanced multiphase liver MRI of diagnostic quality can be performed during free breathing using a combination of compressed sensing, parallel imaging, and golden-angle radial sampling.

Keywords

contrast-enhanced MRI; liver MRI; free-breathing MRI; compressed sensing reconstruction; multicoil compressed sensing reconstruction; golden-angle radial acquisition

Assessment of arterial and venous phases of enhancement is essential for liver lesion detection and characterization.[1,2] Contrast-enhanced multiphase liver magnetic resonance (MR) examination is usually performed using a T1-weighted fat-saturated 3-dimensional (3D) volumetric interpolated sequence with cartesian k-space sampling in a breath hold (BH). However, this method is sensitive to respiratory motion and can result in suboptimal images in patients who cannot adequately hold their breath. Although parallel-imaging and partial-Fourier techniques are usually used for accelerating the examination, this may be insufficient in elderly patients, patients with debilitations, or pediatric patients who have severely limited breath-holding capacity.[3,4] Furthermore, achievable in-plane spatial resolution and anatomic coverage remain limited because of the need to acquire data within a BH.

Recently, a more motion-robust 3D gradient-echo sequence has been developed (radial VIBE) that uses the “stack-of-stars”scheme to acquire volumetric k-space data, where radial sampling is performed in-plane (along k_y and k_x) and cartesian sampling is used along the slice dimension (k_z).[5,6] Studies have shown that free-breathing acquisitions with the stack-of-stars radial VIBE sequence can yield images of comparable image quality with conventional BH examination at the expense of a longer acquisition time.[7,8] This relatively long acquisition time limits its utility for dynamic liver imaging, which requires multiphase acquisitions with temporal resolution of 15 to 20 seconds.

One potential solution to improve the temporal resolution is the application of the compressed sensing (CS) concept, which has recently emerged as a powerful tool for fast imaging by exploiting redundancies in the images.[9] Successful application of CS requires sparsity, incoherence, and nonlinear reconstruction. Magnetic resonance images often can be represented using only few coefficients in an appropriate transform basis. Multiphase liver MRI is a perfect candidate for CS because of extensive spatiotemporal data correlations that result in sparse representations. Compressed sensing can be synergistically combined with parallel imaging to further increase imaging speed.[10–12]

High level of incoherence can be achieved by using irregular k-space sampling patterns. Radial sampling of k-space compares favorably with conventional cartesian schemes for CS because of the inherent presence of incoherent aliasing artifacts from undersampled radial trajectories,[10] which are essential for application of the CS reconstruction. We have recently developed a reconstruction technique that combines CS with parallel imaging for radially acquired dynamic MRI.[13] Two different types of radial acquisition schemes are investigated in this study: the interleaved angle-bisection scheme and the golden-angle scheme, which mainly differ in the temporal order of the k-space sampling. With the interleaved angle-bisection scheme, radial spokes are acquired at a regular angular distance (Fig. 1) in multiple interleaves, such that all spokes from 1 interleave intersect the spokes from the previously acquired interleave.[14] With the recently proposed golden-angle acquisition scheme, on the other hand, the angle of the acquired spokes is continuously increased by 111.25 degrees during the acquisition, resulting in a series of complementary radial spokes with large

angular distance that, for an arbitrary number of spokes, always add up to an approximately uniform angular coverage of the k-space[15] (Fig. 1).

The purposes of this study were to demonstrate the feasibility of performing free-breathing multiphase liver MRI using a combination of CS and parallel imaging with golden-angle (golden-angle radial sparse parallel [GRASP]) and interleaved-angle (interleaved-angle radial sparse parallel [IARASP]) radial sampling scheme and to compare image quality of GRASP and IARASP with conventional BH T1-weighted gradient-echo imaging with cartesian sampling (volumetric interpolate breath hold examination [BH-VIBE]) in healthy participants with normal breath-holding capacity.

MATERIALS AND METHODS

Patient Population

This Health Insurance Portability and Accountability Act–compliant prospective single-center study was performed after obtaining approval from our institutional review board. All participants provided written informed consent. Eight healthy men (mean age, 30.9 years; range 24–41 years) were recruited from a volunteer database at our institution, and each participant underwent MR examination on 3 separate visits (mean delay between consecutive visits, 42 days; range, 31–54 days) on a single 3-T MRI system from October 2010 to December 2011. The order of the acquisition scheme was randomized.

Data Acquisition

Magnetic resonance imaging was performed in all participants on a 3-T clinical system (MAGNETOM Verio; Siemens Healthcare, Erlangen, Germany) using body and spine phased-array coils with 15 elements. All participants underwent 3 separate fat-suppressed T1-weighted gradient-echo contrast-enhanced examinations after injection of gadopentetate dimeglumine (Magnevist, Bayer Healthcare). Dynamic injection of 10-mL Magnevist was administered via a power injector (Spectris; Medrad, Pittsburgh, PA) at a rate of 2 mL/s, followed by a 20-mL saline flush also at a rate of 2 mL/s. All acquisitions were performed with matching sequence parameters, where possible: slice thickness, 3 mm; flip angle, 12 degrees; field of view, 400 × 400 mm^2; image matrix, 256 × 256; partial Fourier along the slice-encoding dimension; spatial resolution, 1.6 × 1.6 × 3 mm^3; repetition time/echo time, 3.56 to 3.62 milliseconds/1.51 to 1.55 milliseconds, 80 partitions (interpolated); and bandwidth, 590 to 610 Hz/voxel. Additional specific details of each acquisition scheme are as follows:

1. Conventional BH-VIBE—A 1-mL test bolus was administered to determine the time-to-peak (TTP) arterial enhancement of the aorta at the level of the celiac artery. Arterial phase imaging was initiated with a delay equal to the TTP, and the venous phase was imaged with a delay of 50 to 60 seconds. A parallel imaging acceleration factor of 2 and partial Fourier were used along the phase-encoding dimension (k_y), resulting in an acquisition time of 14 seconds for each phase.

2. Free-breathing interleaved angle-bisection scheme—A total of 400 radial spokes were acquired using 4 interleaved rotations (100 spokes per rotation) in 60 seconds. The acquisition was initiated, similar to the BH-VIBE acquisition, with a scan delay equal to the TTP arterial enhancement (calculated from a test bolus acquisition that was performed again, as discussed previously). The acquisition was performed with the hands held above the head to decrease streak artifacts from incomplete fat suppression in the upper extremity.

3. Free-breathing continuous golden-angle acquisition—A total of 600 radial spokes were acquired continuously in 90 seconds using the golden-angle scheme. In this case, imaging was initiated at the time of contrast injection without prior timing run or scan delay, which is possible because the golden-angle scheme allows for retrospective selection of timings. The examination was performed with the hands held above the head.

Image Reconstruction

1. Conventional BH-VIBE data sets were reconstructed in-line using the Generalized Autocalibrating Partially Parallel Acquisition reconstruction algorithm.[16]
2. Multicoil CS reconstruction

Interleaved angle-bisection and golden-angle radial acquisitions were reconstructed (IARASP and GRASP, respectively) using radial k-t SPARSE-SENSE method[13] where all slices were processed separately after applying FFT along the k_z dimension. For both schemes, 100 consecutive spokes were grouped into a single temporal frame, yielding 4 temporal frames for IARASP and 6 temporal frames for GRASP. Because the IARASP acquisition was initiated with a scan delay equal to TTP, the first temporal frame (constructed from spokes 1 through 100) constituted the arterial phase and the last frame (spokes 301 through 400; TTP + 45 seconds) constituted the venous phase (Fig. 2A). The GRASP acquisition was initiated at the time of contrast injection; therefore, the first temporal frame (spokes 1 through 100) constituted a precontrast acquisition. The second frame (spokes 101 through 200) acquired with a delay of 15 seconds (similar delay as TTP) after the contrast injection constituted the arterial phase, and spokes 401 to 500 acquired 45 seconds after arterial phase initiation constituted the venous phase (Fig. 2B).

The radial k-t SPARSE-SENSE reconstruction technique combines CS and parallel imaging by enforcing joint sparsity on the multicoil model.[11] Using this approach, additional spatial encoding capabilities of multiple receiver coils are incorporated to further reduce aliasing artifacts associated with undersampling, which enables higher acceleration rates. The reconstruction algorithm aims to minimize the following cost function:

$$D(\mathrm{x}) = \|\mathrm{E} \quad \mathrm{x} - \mathrm{y}\|_2^2 + \lambda \mathrm{T}(\mathrm{x})_1, \quad (1)$$

where **x** is the dynamic image (time series of 3D images) to reconstruct, **E** is the multicoil encoding matrix given by the concatenation of single coil encoding models ($\mathrm{E} = \begin{bmatrix} \mathrm{FS}_1 \\ \vdots \\ \mathrm{FS}_{N_C} \end{bmatrix}$, where **F** is the non-uniform fast Fourier transform defined on the radial trajectory, $\mathbf{S}_1$ is the coil sensitivity matrix for the *l*-th coil, and N_c is the number of coils), **y** is the acquired multicoil k-space data $\left(\mathrm{y} = \begin{bmatrix} \mathrm{y}_1 \\ \vdots \\ \mathrm{y}_{N_c} \end{bmatrix} \right)$, $\| \cdot \|_2$ is the euclidean l_2-norm given by the square root of the sum of square absolute values of the vector, and T is the total variation operator along the temporal domain.[10,11] The term on the right side enforces spatiotemporal sparsity by minimizing the variation between temporal frames, and the term on the left side enforces consistency with the data received by all coils. Note that multicoil sparsity is enforced because **x** represents the contribution from all coils. λ is a regularization parameter that controls the trade-off between spatiotemporal sparsity and data consistency. The reconstruction was implemented in MATLAB (The MathWorks, Natick, MA) using an iterative nonlinear conjugate gradient algorithm. Before the reconstruction, coil sensitivity maps were calculated according to the adaptive coil-combination method[17] where a

composite image that represents the temporal mean of the undersampled data reconstructed with the nonuniform fast Fourier transform was used as coil-calibration reference. The value of λ was decreased during the conjugate gradient iterations where a fixed start value and decrement were used for all data sets, which provided similar results to the time-consuming procedure of finding an optimal λ for each data set. Images were saved in the Digital Imaging and Communications in Medicine (DICOM) format after the reconstruction.

Image Analysis

Arterial and venous enhancement phase images from all examinations were stripped of patient and acquisition parameter details. The images were presented in random order to 2 board-certified radiologists (A.R.,R.L.) with 4 and 6 years of abdominal MRI experience, who evaluated all (DICOM) images independently using a stand-alone workstation.

For each data set, each reader independently scored whether the enhancement pattern of the liver was arterial or venous. Quality of enhancement (QE) was rated subjectively on a 5-point scale (Table 1) on the basis of expected enhancement of the liver in each phase by the experienced readers. Subsequently, the following parameters of image quality were scored using a scale of 1 to 5, with the highest score indicating the most desirable examination (Table 1): overall image quality (IQ), liver edge sharpness (HES), hepatic vessel clarity (HVC), and streak artifact.

Statistical Analysis

The analyses were stratified by phase (arterial vs venous). This was made necessary by the fact that the combined data did not permit a valid test of the interaction between phase and acquisition, and it was considered unreasonable to analyze the combined data under the assumption that any differences among acquisitions were independent of the phase. The individual acquisitions were compared with respect to the mean level of each image quality assessment using mixed model analysis of variance. A separate mixed-model analysis was conducted for each measure, using that measure as the dependent variable. Each mixed model included acquisition type and reader identification as fixed classification factors. Mixed model regression was used to assess the association of IQ with enhancement quality, edge sharpness, HVC, and streak artifact adjusting for reader and acquisition. The covariance structure was modeled by assuming observations to be correlated only when acquired from the same participant and by allowing the error variance to differ across acquisition types. The P values for the comparison of acquisition types are reported with Tukey's honestly significant difference multiple comparison correction. Statistical significance was defined as $P < 0.05$. SAS version 9.3 (SAS Institute, Cary, NC) was used for all computations.

RESULTS

All participants tolerated the MR examinations and performed adequate breath-hold for the conventional BH acquisitions. Each of the 8 participants underwent 3 separate acquisitions, and all examinations were used to generate arterial and venous phase enhancement data sets for each participant. Hence, 48 data sets were reviewed by each reader.

Qualitative Evaluation

Arterial Phase—There was a nominally higher arterial quality of enhancement (QE) score with BH-VIBE compared with GRASP, but this did not reach statistical significance ($P = 0.06$); whereas IARASP had a significantly lower QE score compared with both BH-VIBE and GRASP ($P < 0.005$; Table 2; Fig. 3, A and B). Examinations of BH-VIBE had a significantly higher arterial IQ score compared with those of GRASP and IARASP ($P <$

0.0001). GRASP arterial acquisitions had the second highest IQ score, and this was significantly higher compared with IARASP ($P < 0.0001$). Both readers scored GRASP arterial acquisitions as having an IQ score of acceptable diagnostic quality or better (≥3) in all participants (Fig. 4). BH-VIBE had a significantly higher score for HES and HVC compared with those of GRASP and IARASP ($P < 0.0001$). GRASP arterial acquisitions had a higher score compared with those of IARASP, and this was significant for HVC ($P < 0.0001$) but not for HES ($P = 0.47$). Streak artifacts were also significantly lower with GRASP reconstructions compared with those of IARASP ($P = 0.0005$).

The IQ of the arterial phase images had a significant ($P = 0.0254$) partial correlation ($r = 0.32$) with HVC after adjusting for reader and acquisition. There were no other significant associations between the arterial phase IQ score and other measures of image quality.

Venous Phase—There was a nominally higher venous QE score with BH-VIBE compared with GRASP, but this did not reach statistical significance ($P = 0.07$); whereas IARASP had a significantly lower QE score compared with BH-VIBE and GRASP ($P < 0.05$; Table 3; Figure 3C, D). Examinations of BH-VIBE had a significantly higher venous IQ score compared with those of GRASP and IARASP ($P \leq 0.005$). GRASP acquisitions had the second highest IQ score, and this was significantly higher compared with those of IARASP ($P = 0.0001$). Both readers scored venous phase GRASP acquisitions as having an IQ score of acceptable diagnostic quality or better (≥3) in all participants (Fig. 5). Furthermore, all participants were scored to have IQ score of either good or excellent (≥4), except in 1 participant by reader 2. There was no significant difference in HES between BH-VIBE and GRASP ($P = 0.09$) and between GRASP and IARASP ($P = 0.09$). Examinations of BH-VIBE had a significantly higher score for HVC compared with those of GRASP and IARASP ($P \leq 0.0001$), and GRASP had significantly higher score compared with IARASP ($P = 0.02$). Streak artifacts were significantly lower with GRASP compared with IARASP ($P = 0.004$).

There were no significant associations ($P > 0.1$) between the venous phase IQ score and other image quality parameters.

DISCUSSION

Our results demonstrate that contrast-enhanced multiphase liver MRI during free breathing is feasible using golden-angle radial k-space sampling together with a temporally constrained multicoil CS reconstruction. Slightly lower image quality for the arterial phase compared with the venous phase is likely related to increased streak artifacts from the rapid change in signal intensity in the aorta and the liver from arrival of the bolus of gadolinium contrast, but, in all cases, images were scored as acceptable or better image quality for both phases of enhancement.

Radial acquisition schemes are more motion robust than the conventional rectilinear k-space sampling, which allows for free-breathing acquisition.[7] With cartesian sampling, the respiratory motion disturbs the constant phase offsets among sampled lines, which can be interpreted as displacing individual lines along the phase-encoding direction. Therefore, the Nyquist theorem is violated, leading to the appearance of dominant aliasing effects or “ghosting.” With the radial scheme, every spoke has a different readout direction; hence, this problem is eliminated, and motion artifacts instead present as mild blurring or radially oriented streaks. In addition, the overlap of the spokes in the k-space center averages the object information in time and reduces sensitivity to motion and flow.

We investigated 2 different radial acquisition strategies in our work. The more recently introduced golden-angle scheme yielded consistently higher quality of enhancement and image quality scores compared with the interleaved angle-bisection scheme, both in the arterial- and venous-phase reconstructions. Furthermore, streak artifacts were significantly decreased with GRASP, which can be attributed to the higher temporal incoherence for the acquired k-space data. With golden-angle sampling, each spoke is acquired at a large angular distance from the previous spoke, which causes randomly flickering patterns for undersampled acquisitions. These flickering patterns, in contrast to the object itself, cannot be represented by sparse coefficients in the temporal total variation basis. Thus, stronger discrepancy between the undersampling artifacts and the object representation in the temporal total variation domain results in better image quality and higher effective, achievable acceleration rate for the GRASP approach.

The golden-angle scheme has additional benefits over the interleaved angle-bisection acquisition scheme. With the golden-angle sampling, any number of sequentially acquired spokes result in approximately uniform angular coverage; thus, it provides freedom in reconstructing images retrospectively starting from any spoke and with variable temporal resolution. This has important implications for multiphase liver imaging in patients because it can obviate the need for either a timing run or bolus chase acquisition as well as the need to make a priori assumption on the required temporal resolution. With GRASP, it is not possible to “miss” the arterial phase because a robust arterial phase can always be obtained from the continuously acquired data by retrospectively adjusting the reconstruction window. Furthermore, the ability to reconstruct the acquired data at very high temporal resolution using only a small number of radial spokes for every temporal frame will potentially enable high-resolution free-breathing perfusion imaging of the liver and the upper abdomen in the future,[18] without additional contrast injection or acquisition time. In addition, potential advantages of free-breathing GRASP include the ability to image with higher in-plane spatial resolution and with thinner partitions to obtain near-isotropic resolution without the current imaging constraints of a BH.

In our study, all healthy participants were deemed to be adequate breath-holders and, in almost all cases, the images acquired with the conventional breath-holding approach were of excellent diagnostic quality. However, in patient populations who are sick, elderly, or children, may have difficulty in holding their breath for more than 10 to 15 seconds, resulting in contrast-enhanced images that may be nondiagnostic. In these patient populations, free-breathing GRASP can serve as an alternative to conventional breath-holding techniques in providing diagnostic-quality multiphase imaging of the liver and the upper abdomen.

Our study has several limitations. We imaged a small number of participants ($n = 8$), and imaging was performed in healthy volunteers who may have more regular breathing patterns compared with patients. Furthermore, radial acquisitions were performed with the hands above the head to avoid streak artifacts that sometimes propagate from the outer extremities when the fat saturation is poor in these areas, whereas BH-VIBE acquisition was performed with the hands on the patient's side (similar to the one performed during routine clinical liver examination) because it is more comfortable. Clinical utility and advantage of this technique in patients who cannot adequately hold their breath, for evaluation of focal liver lesions, need to be validated. However, the purposes of this initial study were to introduce a new method for free-breathing dynamic liver MRI using a combination of CS, parallel imaging, and golden-angle radial sampling, and to demonstrate its feasibility.

In conclusion, we have shown that it is possible to perform contrast-enhanced multiphase liver MRI during free breathing with diagnostic image quality using GRASP, a combination

of CS, parallel imaging, and golden-angle radial sampling. In patient populations who have difficulty in holding their breath longer than 10 to 15 seconds, this technique may be a valuable imaging strategy and may help to significantly reduce failure rates by overcoming many of the shortcomings of conventional dynamic abdominal and liver MRI.

Acknowledgments

Supported by grant NIH R01 EB000447 from the National Institutes of Health.

REFERENCES

1. Elsayes KM, Narra VR, Yin Y, et al. Focal hepatic lesions: diagnostic value of enhancement pattern approach with contrast-enhanced 3D gradient-echo MR imaging. Radiographics. 2005; 25:1299–1320. [PubMed: 16160113]
2. Quillin SP, Atilla S, Brown JJ, et al. Characterization of focal hepatic masses by dynamic contrast-enhanced MR imaging: findings in 311 lesions. Magn Reson Imaging. 1997; 15:275–285. [PubMed: 9201674]
3. Paling MR, Brookeman JR. Respiration artifacts in MR imaging: reduction by breath holding. J Comput Assist Tomogr. 1986; 10:1080–1082. [PubMed: 3782557]
4. Maki JH, Chenevert TL, Prince MR. The effects of incomplete breath-holding on 3D MR image quality. J Magn Reson Imaging. 1997; 7:1132–1139. [PubMed: 9400859]
5. Lin W, Guo J, Rosen MA, et al. Respiratory motion-compensated radial dynamic contrast-enhanced (DCE)-MRI of chest and abdominal lesions. Magn Reson Med. 2008; 60:1135–1146. [PubMed: 18956465]
6. Song HK, Dougherty L. Dynamic MRI with projection reconstruction and KWIC processing for simultaneous high spatial and temporal resolution. Magn Reson Med. 2004; 52:815–824. [PubMed: 15389936]
7. Chandarana H, Block TK, Rosenkrantz AB, et al. Free-breathing radial 3D fat-suppressed T1-weighted gradient echo sequence: a viable alternative for contrast-enhanced liver imaging in patients unable to suspend respiration. Invest Radiol. 2011; 46:648–653. [PubMed: 21577119]
8. Azevedo RM, de Campos RO, Ramalho M, et al. Free-breathing 3D T1-weighted gradient-echo sequence with radial data sampling in abdominal MRI: preliminary observations. AJR Am J Roentgenol. 2011; 197:650–657. [PubMed: 21862807]
9. Lustig M, Donoho D, Pauly JM, et al. The application of compressed sensing for rapid MR imaging. Magn Reson Med. 2007; 58:1182–1195. [PubMed: 17969013]
10. Block KT, Uecker M, Frahm J, et al. Undersampled radial MRI with multiple coils: iterative image reconstruction using a total variation constraint. Magn Reson Med. 2007; 57:1086–1098. [PubMed: 17534903]
11. Otazo R, Kim D, Axel L, et al. Combination of compressed sensing and parallel imaging for highly accelerated first-pass cardiac perfusion MRI. Magn Reson Med. 2010; 64:767–776. [PubMed: 20535813]
12. Vasanawala SS, Alley MT, Hargreaves BA, et al. Improved pediatric MR imaging with compressed sensing. Radiology. 2010; 256:607–616. [PubMed: 20529991]
13. Chandarana, H.; Feng, L.; Block, TK., et al. Free-breathing dynamic contrast-enhanced MRI of the liver with radial golden-angle sampling scheme and advanced compressed-sensing reconstruction.. Proceedings of the 20th Annual Meeting of the ISMRM; Melbourne, Australia. 2012;
14. Song HK, Dougherty L. k-Space weighted image contrast (KWIC) for contrast manipulation in projection reconstruction MRI. Magn Reson Med. 2000; 44:825–832. [PubMed: 11108618]
15. Winkelmann S, Schaeffter T, Koehler T, et al. An optimal radial profile order based on the golden ratio for time-resolved MRI. IEEE Trans Med Imaging. 2007; 26:68–76. [PubMed: 17243585]
16. Griswold MA, Jakob PM, Heidemann RM, et al. Generalized autocalibrating partially parallel acquisitions (GRAPPA). Magn Reson Med. 2002; 47:1202–1210. [PubMed: 12111967]
17. Walsh DO, Gmitro AF, Marcellin MW. Adaptive reconstruction of phased array MR imagery. Magn Reson Med. 2000; 43:682–690. [PubMed: 10800033]

18. Chandarana, H.; Feng, L.; Block, TK., et al. Contrast-enhanced free-breathing perfusion weighted MR imaging of the whole-liver with high spatial and temporal resolution.. Proceedings of the 20th Annual Meeting of the ISMRM; Melbourne, Australia. 2012;

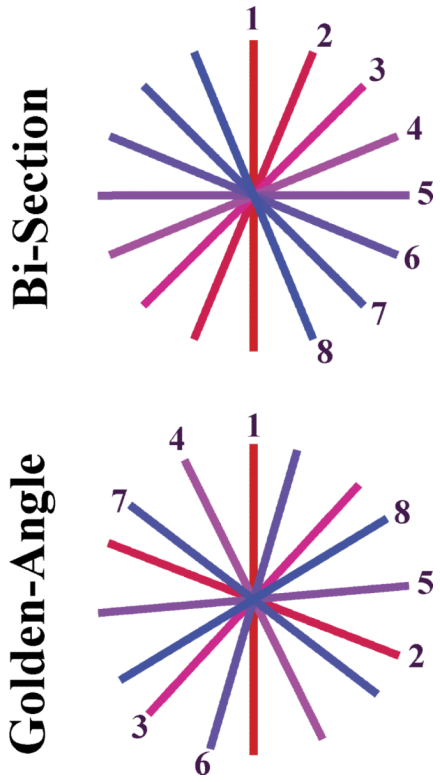

FIGURE 1.
Schematic of sampling scheme for interleaved angle-bisection and continuous golden-angle acquisitions. Temporal frames in the bisection scheme need to be predefined, whereas the golden-angle scheme provides freedom in defining temporal frames retrospectively by grouping any different number of consecutive spokes.

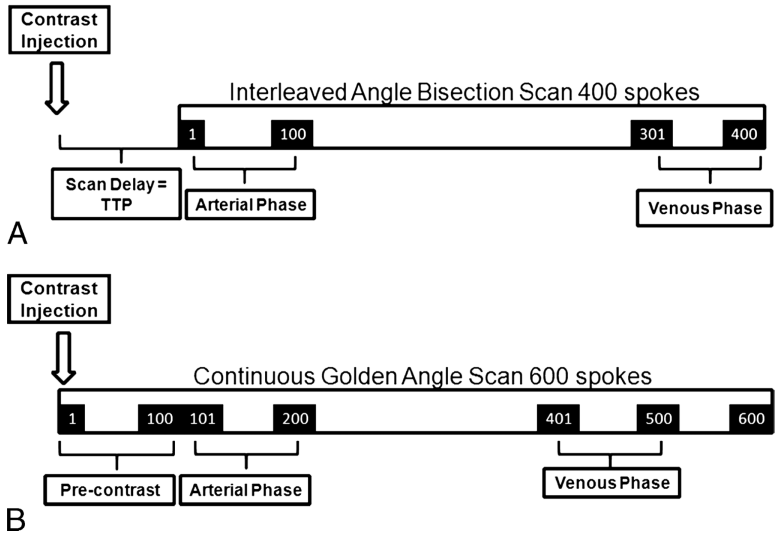

FIGURE 2.

Schematic of IARASP reconstruction for interleaved angle-bisection acquisition scheme (A) and GRASP reconstruction

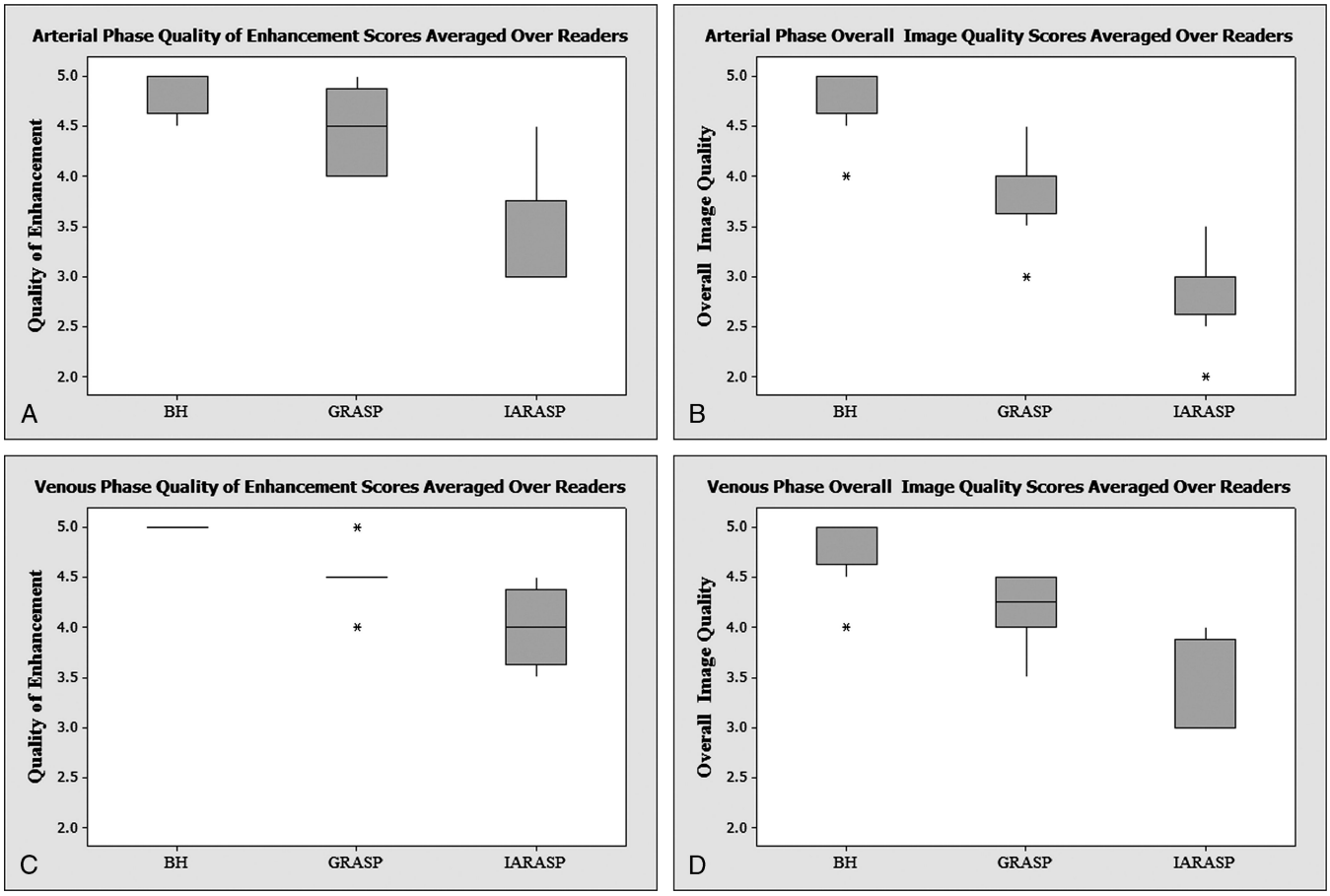

FIGURE 3.

Box plot of QE arterial phase (A), IQ arterial phase (B), QE venous phase (C), and IQ venous phase (D) averaged over readers for conventional BH-VIBE, GRASP, and IARASP.

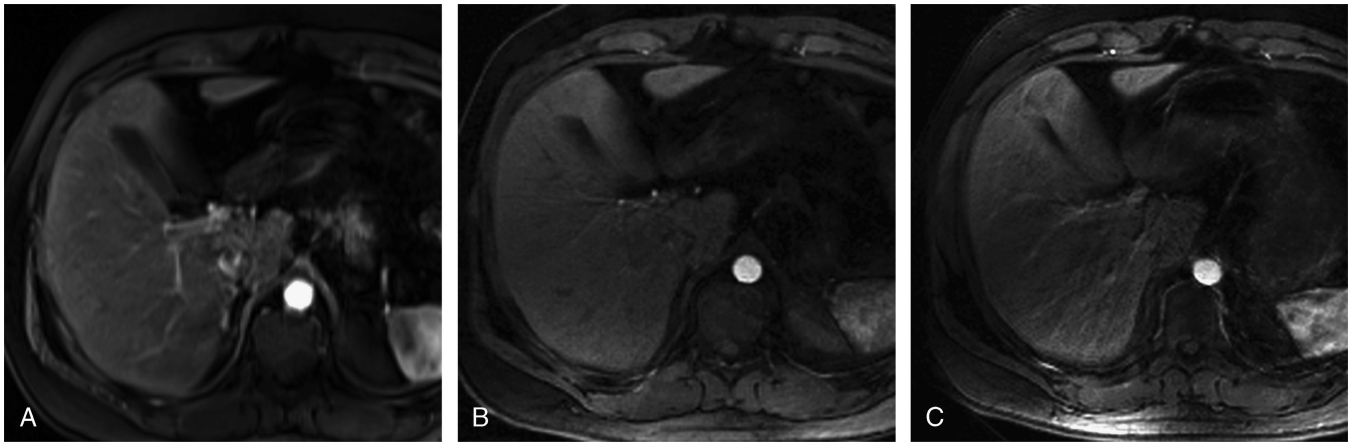

FIGURE 4.
Images taken from a 32-year-old man who underwent 3 separate examinations of the liver after contrast administration. Arterial phase BH-VIBE (A), GRASP (B), and IARASP (C) reconstructions. BH-VIBE received an IQ score of 5, GRASP was scored as 4, and IARASP was scored as 3. BH-VIBE received a QE score of 5, GRASP was scored as 4, and IARASP was scored as 3.

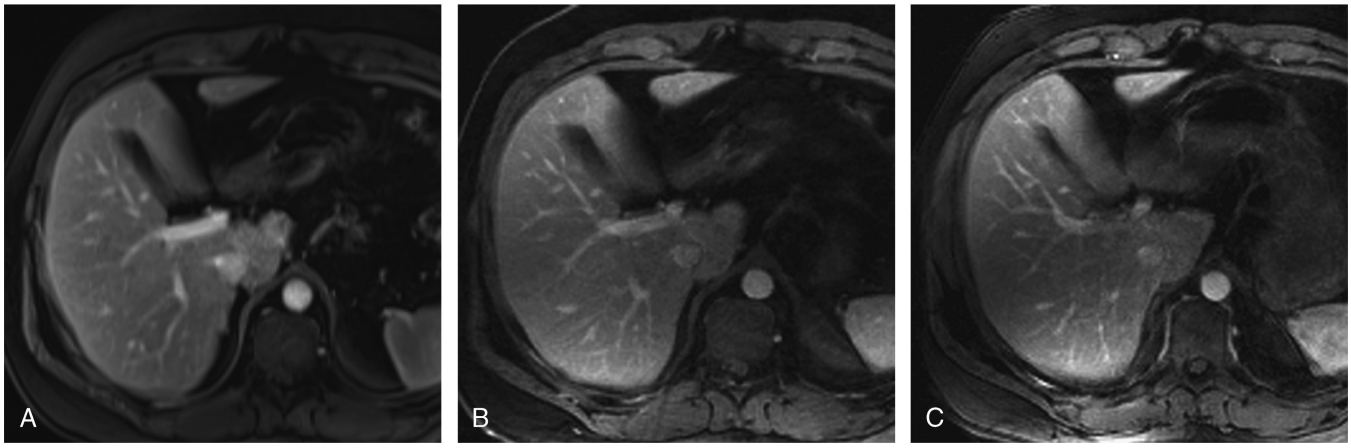

FIGURE 5.
Images taken from a 32-year-old man who underwent 3 separate examinations of the liver after contrast administration. Venous phase BH-VIBE (A), GRASP (B), and IARASP (C) reconstructions. GRASP and BH-VIBE received an IQ score of 5, which was higher than IARASP, which received a score of 4. BH-VIBE and GRASP received a QE score of 5, and IARASP was scored as 4.

TABLE 1

Scoring System of Image Quality Parameters

Image Quality Parameter	Score	Scoring System
Quality of enhancement	1–5	1, unacceptable; 2, poor; 3, acceptable; 4, good; and 5, excellent
Overall image quality	1–5	1, unacceptable; 2, poor; 3, acceptable; 4, good; and 5, excellent
Liver edge sharpness and hepatic vessel clarity	1–5	1, unreadable; 2, extreme blur; 3, moderate blur; 4, mild blur; and 5, no blur
Streak artifact	1–5	1, unreadable; 2, extreme artifact; 3, moderate artifact; 4, mild artifact; and 5, no artifact

TABLE 2

Image Quality Parameter Scores for Arterial Phase Acquisitions Averaged Over All Participants and Both Readers (Part A) and *P* values for Comparison of Image Quality Parameters Between the 3 Acquisition Schemes (Part B)

Part A[*]

Sequence	BH	GRASP	IARASP
QE	4.9 (0.3)	4.4 (0.5)	3.3 (0.6)
IQ	4.8 (0.4)	3.9 (0.5)	2.9 (0.5)
HES	4.9 (0.3)	3.9 (0.8)	3.5 (0.7)
HVC	4.8 (0.5)	3.5 (0.5)	2.8 (0.7)
Streak artifact	5.0 (0.0)	3.6 (0.6)	2.7 (0.7)

Part B[†]

QE / HES	IQ / HVC	GRASP		IARASP	
BH-VIBE		0.06	<0.0001	<0.0001	<0.0001
		<0.0001	<0.0001	<0.0001	<0.0001
GRASP				<0.0001	<0.0001
				0.47	<0.0001
IARASP					

[*] All values are expressed as mean (SD) where a score of 1 is unacceptable and a score of 5 is excellent.

[†] Key in the upper left-hand corner indicates *P* values for each image quality parameter.

TABLE 3

Image Quality Parameter Scores for Venous Phase Acquisitions Averaged Over All Participants and Both Readers (Part A) and *P* values for Comparison of Image Quality Parameters Between the 3 Acquisition Schemes (Part B)

Part A[*]

Sequence	BH	GRASP	IARASP
QE	5 (0.0)	4.5 (0.5)	4.0 (0.5)
IQ	4.8 (0.4)	4.2 (0.5)	3.3 (0.5)
HES	5 (0.0)	4.4 (0.7)	4.3 (0.6)
HVC	4.9 (0.3)	4.0 (0.6)	3.4 (0.6)
Streak artifact	5.0 (0.0)	3.8 (0.4)	3.3 (0.5)

Part B[†]

QE / HES	IQ / HVC	GRASP		IARASP	
BH-VIBE		0.07	0.005	<0.0001	<0.0001
		0.09	0.0001	<0.0001	<0.0001
GRASP				0.048	0.0001
				0.09	0.02
IARASP					

[*] All values are expressed as mean (SD) where a score of 1 is unacceptable and a score of 5 is excellent.

[†] Key in the upper left-hand corner indicates P values for each image quality parameter.